Spatial and temporal scaling of sub-daily extreme rainfall for data sparse places

R. L. Wilby[1] · C. W. Dawson[2] · D. Yu[1,3] · Z. Herring[4] · A. Baruch[3] · M. J. Ascott[5] · D. L. Finney[6] · D. M. J. Macdonald[5] · J. H. Marsham[6,7] · T. Matthews[8] · C. Murphy[9]

Abstract

Global efforts to upgrade water, drainage, and sanitation services are hampered by hydrometeorological data-scarcity plus uncertainty about climate change. Intensity–duration–frequency (IDF) tables are used routinely to design water infrastructure so offer an entry point for adapting engineering standards. This paper begins with a novel procedure for guiding downscaling predictor variable selection for heavy rainfall simulation using media reports of pluvial flooding. We then present a three-step workflow to: (1) spatially downscale daily rainfall from grid-to-point resolutions; (2) temporally scale from daily series to sub-daily extreme rainfalls and; (3) test methods of temporal scaling of extreme rainfalls *within* Regional Climate Model (RCM) simulations under changed climate conditions. Critically, we compare the methods of moments and of parameters for temporal scaling annual maximum series of daily rainfall into sub-daily extreme rainfalls, whilst accounting for rainfall intermittency. The methods are applied to Kampala, Uganda and Kisumu, Kenya using the Statistical Downscaling Model (SDSM), two RCM simulations covering East Africa (CP4 and P25), and in hybrid form (RCM-SDSM). We demonstrate that Gumbel parameters (and IDF tables) can be reliably scaled to durations of 3 h within observations and RCMs. Our hybrid RCM-SDSM scaling reduces errors in IDF estimates for the present climate when compared with direct RCM output. Credible parameter scaling relationships are also found within RCM simulations under changed climate conditions. We then discuss the practical aspects of applying such workflows to other city-regions.

Keywords Regional climate downscaling · Extreme rainfall · Intensity–duration–frequency · Tropics · Flood

✉ R. L. Wilby
r.l.wilby@lboro.ac.uk

1 Geography and Environment, Loughborough University, Loughborough LE11 3TU, UK

2 Department of Computer Science, Loughborough University, Loughborough LE11 3TU, UK

3 Previsico, Advanced Technology Innovation Centre, Loughborough LE11 3QF, UK

4 Oakwood, Derby DE21 4BB, UK

5 British Geological Survey, Maclean Building, Crowmarsh OX10 8BB, UK

6 School of Earth and Environment, University of Leeds, Leeds LS2 9JT, UK

7 National Centre for Atmospheric Science, Leeds, UK

8 School of Geography, King's College London, London WC2B 4BG, UK

9 Department of Geography, Irish Climate Analysis and Research Units (ICARUS), Maynooth University, Co. Kildare, Ireland

1 Introduction

Global efforts to upgrade water infrastructure and improve sanitation services are hampered by a lack of hydrometeorological data—especially for rapidly growing cities in the tropics. There is a particular need for information about *sub-daily* extreme rainfall to design hydraulic structures. This demand is heightened by concerns about climate variability and change which are expected to increase the incidence of heavy rainfall and flooding (Westra et al. 2014)—conditions that amplify human health risks (de Magny et al. 2012; Gough et al. 2019; WHO 2018). Although there are numerous techniques for statistically simulating (Kigobe et al. 2011) or downscaling *daily* rainfall (Wilby et al. 1998; Maraun and Widmann 2018), there are limited options for estimating sub-daily extreme rainfalls in data scarce situations (De Paola et al. 2014; Courty et al. 2019; Liew et al. 2014). Furthermore, because of a lack of data, there are few studies of sub-daily rainfall changes at city-scales in the

tropics (Lu and Qin 2020; Herath et al. 2016; Kuok et al. 2016).

Fortunately, considerable advances are being made in the estimation of sub-daily (and even sub-hourly) rainfall intensities from more widely available daily data. This is possible because extreme rainfall statistics are known to scale across different durations (Gupta and Waymire 1990; Olsson et al. 1993; Burlando and Rosso 1996; Svensson et al. 1996; Koutsoyiannis et al. 1998). Various methods exist for temporal scaling but the most widely adopted to date rely on fractal, power-law, ratio, or quantile–quantile scaling techniques (Benestad et al. 2021; Hassanzadeh et al. 2019; Menabde et al. 1999; Nguyen et al. 1998; Silva et al. 2017; Srivastav et al. 2014). Scaling parameters from such models may also be correlated with location-specific variables—such as site distance from coast, elevation, latitude, and longitude—enabling regionalisation and potential estimation for ungauged sites (Rodríguez-Solà et al. 2017; Casas-Castillo et al. 2018). Despite these developments there is still scope for methodological improvement, not least in the treatment of rainfall intermittency which can lead to overestimation of rainfall duration and thereby underestimation of intensities when sub-daily data are aggregated to daily blocks (Dunkerley 2019, 2021).

Scaling techniques are also being used to adjust rainfall intensity–duration–frequency (IDF) tables to reflect climate change. As IDF tables are routinely used to design water infrastructure, they offer a way of adapting engineering standards for changed climate conditions (Agarwal et al. 2021; Butcher et al. 2021; Kristvik et al. 2019; Nguyen et al. 2007; Nguyen and Nguyen 2020; Requena et al. 2021a). The general expectation is that IDF curves will be uplifted and steepened by climate change as the intensity of rare, short-duration storms increase by more than long-duration events (Förster and Thiele 2020; Hosseinzadehtalaei et al. 2020). Some have applied temporal scaling methods to generate hourly extreme rainfalls from daily regional climate model (RCM) simulations (Hanel and Buishand 2010; Lee and Park 2017) or to evaluate the effects of RCM grid resolution, multi-scaling, event duration and return period on model biases (Beranová et al. 2018; Requena et al. 2021b; Sunyer et al. 2017). However, as far as we are aware, we are the first to compare temporally scaled sub-daily extreme rainfalls with directly simulated extremes from RCMs under changed climate conditions—including for an RCM with a convection-permitting scheme. In this way, we test the ability of temporal scaling methods to replicate extreme rainfalls simulated under present and changed climate conditions within RCM runs.

Our study evaluates sub-daily rainfall IDF tables derived from statistically (SDSM) and dynamically (RCM) downscaled daily output under present and changed climate conditions. We apply a three-step workflow to: (1) spatially downscale *daily* rainfall then extract annual maximum series; (2) temporally scale *sub-daily* extreme rainfalls using contrasting methods, with and without an adjustment for rainfall intermittency; and (3) evaluate errors in temporal scaling under present and changed climate conditions using output from two RCMs (with and without convection-permitting schemes). These methods are illustrated for the cities of Kampala, Uganda and Kisumu, Kenya. Throughout, our focus is on methodological testing and advancement rather than on producing climate change projections per se. Furthermore, we demonstrate a new technique for downscaling model calibration by triangulating against newspaper reports of heavy rainfall and urban flooding. Our research also adds to limited knowledge about sub-daily extreme rainfalls for vulnerable cities in the tropics by deploying scaling techniques that require only daily rainfall data.

The next section introduces the test sites and steps taken to quality assure rainfall data. This is followed by a description of the daily and sub-daily downscaling algorithms, including our newspaper method for model calibration which is deliberately weighted towards downscaling heavy rainfall. We then demonstrate the spatial and temporal downscaling techniques using Kampala and Kisumu including an evaluation of errors in simulations of sub-daily extreme rainfalls under present and changed climate conditions. We discuss the results and practical considerations when downscaling extreme rainfalls for design purposes in data scarce places. Finally, we close with some suggestions for further research.

2 Materials and methods

2.1 Study areas

Population growth within the Lake Victoria Basin (LVB) is faster than the continental average for Africa (Drakenberg et al. 2007). Kampala (Uganda) is one of the fastest growing cities in Africa with an annual growth rate of 4.03% (City Mayors 2020); Kisumu (Kenya) is the second largest city in the LVB and likewise growing rapidly (Ananga et al. 2019) (Fig. 1). Although 300 km apart, the mean annual rainfall of the cities is very similar (~ 1400 mm) with 1-day maxima occasionally exceeding 100 mm. Both urban areas have experienced cholera outbreaks linked to recurrent episodes of surface water flooding combined with lack of adequate water supply and sanitation systems (Olago et al. 2007). Hence, authorities have been developing city-scale models to evaluate public health benefits of improved water and sanitation services (Oyoo et al. 2011; Barbosa et al. 2012; Peal et al. 2014).
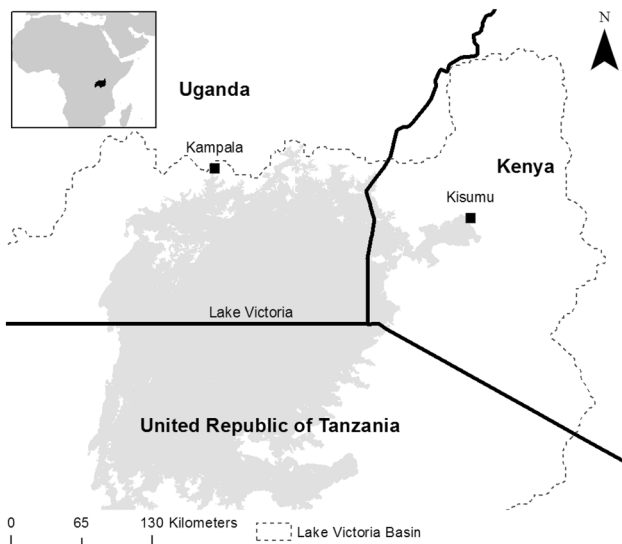
Fig. 1 Location of the study cities. The inset map shows the Lake Victoria Basin

2.2 Rainfall data and quality assurance

Daily rainfall series were obtained for Kampala (Makerere University, 0.334° N, 32.569° E) (1993–2018) and Kisumu (airport, 0.09° S, 34.73° E) (1961–2015) weather stations from the Uganda National Meteorological Authority (UNMA) and the Kenya Meteorological Department (KMD), respectively. Historic IDF tables of extreme rainfall intensities (for 0.25, 0.5, 1, 3 and 6 h durations) are publicly available for both cities (Taylor and Lawes 1971; henceforth T&L). In addition, 15-min rainfall data were recorded by automatic weather stations (henceforth AWS) installed by the HyCRISTAL project (Macdonald et al. 2018) at five sites in Kampala. The most complete record at Kanyanya (0.375° N, 32.583° E) (2017–2021) was used to investigate sub-daily rainfall intermittency and intensity scaling with wet-spell duration.

Given our focus on extreme rainfalls, daily data were quality assured for large outliers, day of week biases, and affinity to round values that are divisible by 5 and 10 (so called "5/10 bias")—all of which potentially distort extreme value estimates (Daly et al. 2007; Viney and Bates 2004). No suspect outliers were identified in the Kampala record as all annual maxima lie within 2.5 standard deviations of the mean. This was not the case for Kisumu. Two values fell outside 7 standard deviations of the mean (292 mm on 30/6/15, 237 mm on 21/7/14); the next largest value (153.3 mm on 13 May 2011) lies within 3.5 standard deviations. The two largest values were subsequently confirmed by KMD as data entry errors with missing decimalization, so corrected to 29.2 mm and 23.7 mm, respectively. However, concerns remain about the integrity of some of the other outliers,

especially those that were not corroborated by newspaper reports of urban flooding (see Sect. 2.3).

According to the Mann–Whitney U-test, both records fail the 5/10 bias test ($p < 0.01$), meaning that there are higher than expected frequencies of daily totals divisible by 5 (Fig. S1). However, closer inspection of the extreme value series reveals that there is only one annual maximum for Kampala (60 mm in 2002) and one for Kisumu (50 mm in 1969) that is divisible by 5. This suggests that the 5/10 bias is present only in more frequently occurring rainfall totals (< 30 mm/day). Single factor Anova-testing shows that neither record exhibits a statistically significant ($p < 0.05$) day of week bias [although Kisumu does have a tendency for high wet-day means at the weekend, perhaps indicating some aggregation of multiple days with rainfall into a single day (Fig. S2)]. The non-parametric Pettitt test applied to annual rainfall totals and wet-day counts reveals no abrupt changes in the mean, although there have been ~ 8% fewer rain days in Kisumu since the early 1970s. Based on these tests, we conclude that the daily records at both sites are reliable for extreme event analysis, but analyses for Kisumu should be interpreted with caution.

2.3 Media reports of flooding

Reports of pluvial flooding were used to quality assure daily rainfall outliers, then to calibrate and evaluate the downscaling model. Following Wells et al. (2016) and Ahadzie and Proverbs (2011), we catalogued reports of floods in both cities by examining online news reports, academic literature, and social media during the period 1988–2016 using the key words: '*flood*', '*rainfall*', '*Kisumu*', '*Kampala*' (see: Supplementary Information, Tables S1 and S2). Archives examined included Google, Google News, Google Scholar, Twitter and YouTube as well as major regional news agencies. The six national newspapers surveyed were: *New Vision*,[1] *The Daily Monitor*,[2] *All Africa*,[3] *Hivisasa*,[4] *Daily Nation*[5] and *The Star*.[6] Online archives of the *Daily Monitor* and *New Vision* were also cross-checked with printed matter but yielded no further reports of flooding. Additionally, some severe flash flood episodes (such as 25 June 2012 and 13 April 2016) captured by our media search are independently corroborated by other studies (Umer et al. 2021, 2022).

Where possible, event dates, locations and associated flood impacts were documented. The media reports covered

[1] https://www.newvision.co.ug/.

[2] http://www.monitor.co.ug/.

[3] http://allafrica.com/.

[4] https://hivisasa.com/.

[5] https://www.nation.co.ke/.

[6] https://www.the-star.co.ke/.

Table 1 Candidate downscaling predictor variables

Code	Description
DSWR	Direct shortwave radiation
LFTX	Surface lifted index (temperature difference between an air parcel lifted adiabatically and the environment at a given height in the atmosphere)
MSLP	Mean sea level pressure
H500	500 hPa geopotential height
H850	850 hPa geopotential height
PTMP	Potential temperature (temperature that an unsaturated air parcel would have if lowered [or raised] to a standard pressure)
PWTR	Precipitable water (depth of water in a column of the atmosphere if all the water in that column were precipitated as rain)
PREC	Precipitation total (comprising total liquid plus solid precipitation)
R500	Relative humidity at 500 hPa height
R850	Relative humidity at 850 hPa height
RHUM	Near surface relative humidity
SHUM	Near surface specific humidity
TEMP	Near surface air temperature

a range of topics, including loss of life, damage to homes and city infrastructure by floodwaters and sewage, contamination of drinking water supplies, outbreaks of waterborne disease and malaria, closure of schools, disruption of transport and businesses; some reflected on underlying exacerbating factors such as city encroachment onto wetland areas, blocked culverts and poor maintenance of drainage systems. However, for the present study, the most important detail was the date of the flood. This was not always the day of the news article—in particular for printed media—so we carefully checked reports to accurately cross-match the flood with antecedent and same-day rainfall totals. Only two news reports were found for Kisumu prior to 2003, so the media analysis for this city was limited to the period 2003–2016.

## 2.4 Statistical downscaling predictor variables and RCM experiments

Daily atmospheric predictor variables were used to calibrate the Statistical DownScaling Model (SDSM) (Wilby et al. 2014). Predictors were obtained from the National Center for Environmental Prediction (NCEP) re-analysis (Kalnay et al. 1996) for the 2.5° grid cell overlying each city, using the common period (1993–2015). The suite of downscaling predictors is available at: https://sdsm.org.uk/data.html. This includes downward shortwave radiation (DSWR), a surface lifting index (LFTX), potential temperature (PTMP), precipitable water (PWTR), and total liquid plus solid precipitation (PREC). These variables were added to the standard SDSM suite to improve downscaling of convection, which is the physical driver of extreme rainfall episodes in the tropics. Due to the proximity of both cities to the equator, the Coriolis force is near zero, so geostrophic airflow components and vorticity were not included. All candidate predictor

variables selected for downscaling model calibration are listed in Table 1. During the calibration procedure, NCEP variables were cross-matched with the dates of the above media reports to identify antecedent and coincident regional atmospheric conditions that were most strongly associated with heavy rainfall and local flooding. Three sets of predictor variables (suites) were used to calibrate SDSM to test sensitivity of the extreme rainfalls to this step in the spatial downscaling model formulation.

Hourly rainfall simulations (for grid cells closest to the cities) were obtained from two RCMs to evaluate temporal downscaling methods under changed climate conditions. The first RCM was the pan-African, convection-permitting 4.5 km resolution simulation (CP4) experiment (Kendon et al. 2019; Stratton et al. 2018). The second was a non-convection-permitting RCM simulation (P25-Africa) using identical resolution and physical parameterizations to the 25 km-resolution global model HadGEM2-ES. Both CP4 and P25 were run for 10-year present (1997–2007) and changed climate (~ year 2100) simulations under RCP8.5 emissions. The global mean temperature change of the global parent model driving both RCMs is 5.2 K relative to 1975–2005 (Kendon et al. 2019). Hence, these change experiments are representative of high-end climate forcing and climate model sensitivity.

Finally, normalized daily precipitation series from both RCMs were used in place of NCEP predictors to drive SDSM. This perfect-prognosis technique assumes that downscaled NCEP-to-local rainfall relationships are the same as the downscaled RCM-to-local rainfall relationship (under present and changed forcing). Until now, neither P25 nor CP4 have been downscaled to the city-scale. However, we stress that these RCM experiments were deployed only for temporal scaling method evaluation—the precipitation

Fig. 2 Overview of the methodological framework and workflow
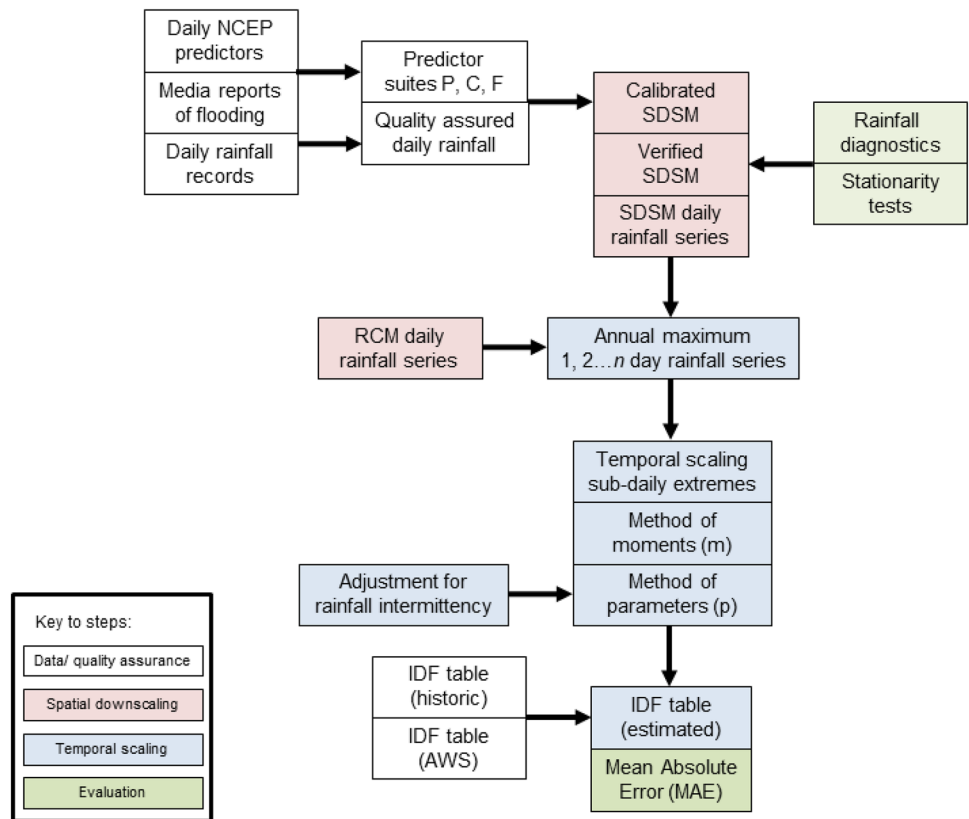
change signals in the CP4 runs for East Africa have been analysed elsewhere (Finney et al. 2019, 2020a).

3 Downscaling daily and sub-daily extreme rainfalls

Having quality assured rainfall data and downscaling model outputs, the workflow proceeds in three steps (Fig. 2). First, spatial downscaling is undertaken via SDSM (using re-analysis predictors) and the two RCMs (P25 and CP4) to simulate daily rainfall series for each city. Second, two temporal scaling methods are used to convert 1- to *n*-day annual maximum rainfall series into sub-daily extreme rainfalls. Third, IDF tables produced by spatial and temporal downscaling are compared with those derived from observations (AWS and T&L) and unscaled hourly rainfall from the RCMs. Each step is described in detail below.

3.1 Step 1: spatial downscaling of daily rainfall

SDSM was used to simulate daily rainfall for Kampala and Kisumu. This tool can bias correct, reconstruct, and infill missing data (even from fragmented meteorological records) to generate multi-decadal series, with confidence intervals. The technical development and applications of SDSM have

been described at length before (Wilby et al. 2002, 2003, 2014; Wilby and Dawson 2013). In summary, SDSM is a conditional weather generator that links atmospheric predictor variables (here originating from NCEP) to time-varying parameters of daily weather at individual sites (here wet-day occurrence and amounts at sites within cities). The procedure for downscaling is either unconditional (as for wet-day occurrence), or conditional on an event (as for rainfall amounts) (Wilby et al. 2014). Model error is assumed to be Gaussian and stochastically generated to give more realistic variance, but this inflation procedure can reduce autocorrelation in downscaled daily series when compared to observations. Nonetheless, the stochastic component does enable simulation of ensembles of time-series that reflect model uncertainty. Previous sensitivity testing shows that at least 10 years of daily data are ideally needed for SDSM calibration (Wilby et al. 2014).

SDSM parameters are obtained via ordinary least squares calibration of the transfer function between regional NCEP predictor variables and the local predictand (here, daily rainfall series). All predictors were normalized by their respective climatological means and standard deviations (i.e., expressed as *z*-scores rather than absolute values). This enables downscaling of similarly normalized predictors from other sources (later, daily precipitation from the RCMs). All regional downscaling methods assume that

Table 2 Downscaling predictor suites tested for Kampala

Suite	NCEP predictors	Description
P	PREC	Based on model physics and parameterizations, NCEP grid-area average precipitation has been shown to outperform conventional downscaling predictor suites (Widmann et al. 2003)
C	LFTX, PWTR, H850	The assumption is made that these predictor variables are well-resolved and realistically simulated by NCEP whilst being strongly correlated with local precipitation (Wilby and Wigley 2000)
F	PTMP, PWTR, RHUM, R500	Candidate variables are initially identified as those with markedly different mean on days with/without floods, thereby highlighting those predictors associated with local, heavy rainfall

predictor-predictand relationships are stationary; local forcings and feedbacks due to, for instance, land-surface changes during the calibration period are not explicitly represented. In practice, the parameters of statistical and dynamical downscaling techniques are known to vary over time, not least because of inter-decadal climate variability (Charles et al. 1999; Wilby 1997). With these points in mind, the stationarity of extreme rainfalls is evaluated in Sect. 4.2.

In addition to model structure, downscaled series are also sensitive to the choice of predictor variables (Crawford et al. 2007; Borges et al. 2017). Other work warns about equifinality and transferability issues—whereby alternative predictor sets yield equivalent skill during model calibration and validation but different projections when applied under changed climate conditions (Fu et al. 2018). To assess predictor uncertainty, three suites of downscaling variables were tested (Table 2): (i) NCEP (and later RCM) precipitation as the only predictor (set P); (ii) conventional predictors informed by physical considerations such as atmospheric stability, moisture content, and thickness (set C); and (iii) flood-informed predictors guided by coincident media reports (set F). Suite F was determined by stratifying daily NCEP predictors (Table 1) into days before, during, and without media reports of pluvial flooding in Kampala, then identifying those variables that exhibit largest absolute differences in the mean and/or sign. Finally, this sub-set was reduced to those variables with the highest partial correlations, and all model variants were evaluated against a set of rainfall diagnostics (Haylock et al. 2006).

3.2 Step 2: temporal scaling of sub-daily extreme rainfalls for the present climate

There are broadly two groups of statistical technique for temporal downscaling rainfall: those that generate synthetic series based on quasi-mechanistic representations of sub-daily stochastic rainfall processes, and those that implement (multi-)scaling procedures founded on fractal theory (Onof et al. 2000). The second group of models are relatively parsimonious and, amongst these, two require only daily rainfall data for their calibration: (1) the method of moments; and (2) the method of parameter

scaling. Both are implemented within the latest version of SDSM, and both methods were used to scale AWS, station, SDSM, CP4 and P25 daily data to sub-daily extreme rainfalls. Bias correction was applied to the RCMs to enable fairer comparison between SDSM (point estimates) and RCM (grid estimates). This was simply based on the ratio between the mean annual maximum 24 h intensity in the RCM and station data so as to not constrain the sub-daily rainfall estimates produced from RCMs.

3.2.1 Method of moments

The method of moments rests on the assumption that rainfall intensities scale according to the power law over durations of 0.5–24 h (Menabde et al. 1999). This model has been applied widely and takes the form:

$$I_{t,T} = I_{24,T}\left(\frac{t}{24}\right)^{\eta} \tag{1}$$

where I is the sub-daily maximum rainfall intensity (mm/h) over duration t (h) with return period T (years). Daily maximum rainfall intensities $I_{24,T}$ for return periods 2, 5, 10, and 20 years are obtained from the Gumbel distribution fit to annual maximum series of 24 h intensities. The scaling parameter η was estimated by first regressing the non-central moments λ of order q of the annual maximum series of intensities I_t^q against t; then second, regressing the resulting coefficients $K(q)$ against q where

$$I_t^q = \lambda^{K(q)} I_{24}^q \tag{2}$$

$$K(q) = \eta q \tag{3}$$

The parameter η is typically derived from sub-daily rainfall data. However, some studies show that the scaling relationship holds over one, and even up to three weeks (García-Marín et al. 2013; Rodríguez-Solà et al. 2017). The upper limit d_u (days) of scaling depends on site-specific synoptic weather conditions. Sensitivity testing of simulated IDF tables to d_u over the range 2–15 days, suggests optimal values in the region of 2–4 days for Kampala and Kisumu (Fig. 3).
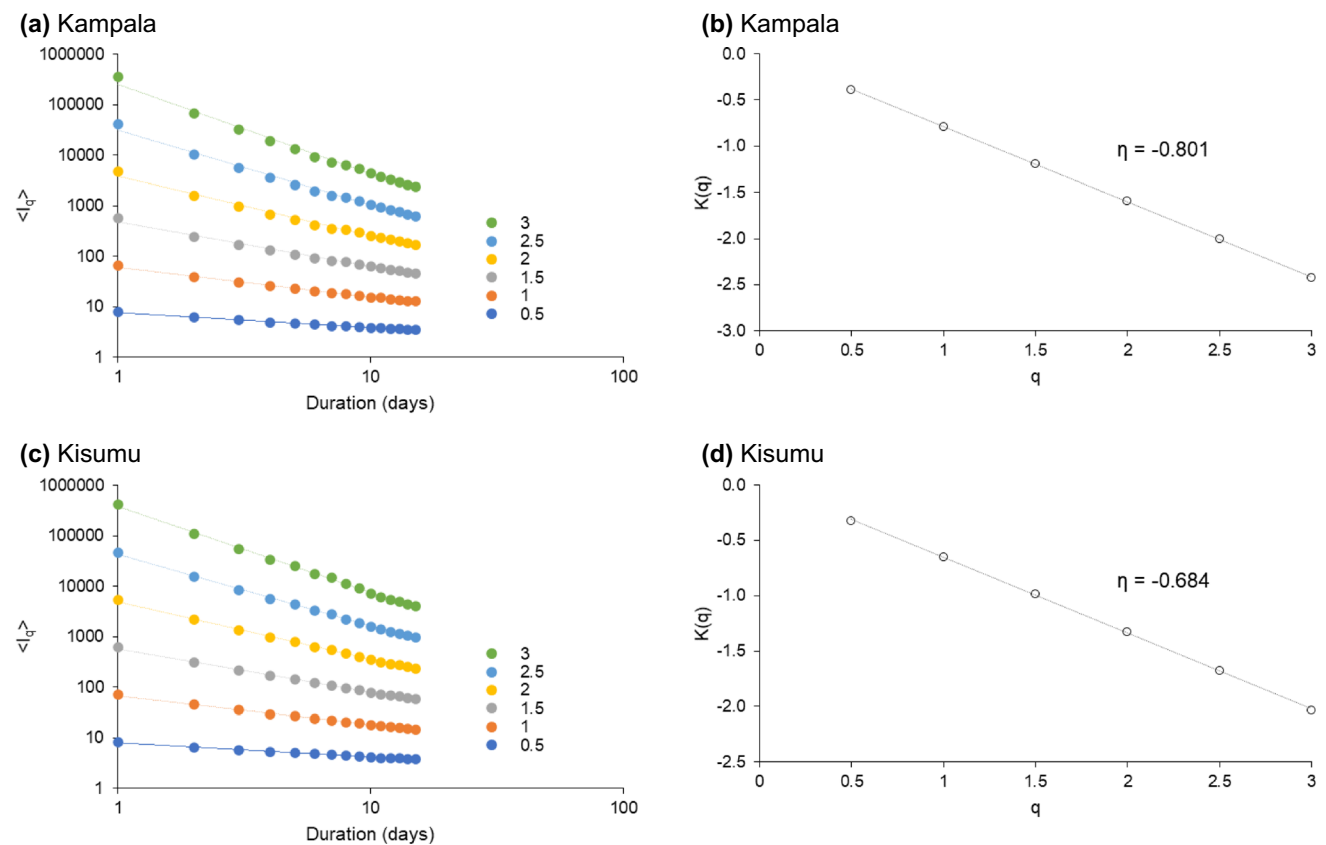
Fig. 3 Statistical moments of observed rainfall intensity ($<I_q>$) derived from annual maximum series over durations of 1–15 days at **a** Kampala and **c** Kisumu for the period 1993–2015. The scale function $K(q)$ shows the relationship between the gradients between $<I_q>$ and duration (in **a** and **c**) with respect to the moment (q) at **b** Kampala and **d** Kisumu. See Sect. 3.2.1 for an explanation of the method of moments

3.2.2 Method of parameter scaling

Following Menabde et al. (1999) and Bougadis and Adamowski (2006), we fit the Gumbel distribution (location μ, scale σ) to annual maximum series. Gumbel was used to maximise parsimony but SDSM can also fit the GEV distribution. However, rather than using annual maxima of sub-daily rainfall intensities, we estimate Gumbel parameters using annual maxima of n-day totals accumulated over $n=1, 2, 3,\ldots,$ 15 days (i.e., $d=24, 48, 72,\ldots, 360$ h). As in Overeem et al. (2008), we assume that the μ and σ parameters depend on duration—an assumption supported by AWS data (Fig. 4). Power and linear scaling of Gumbel parameters were tested and the former found to produce the best least squares fit as:

$$\mu_t = c\mu_a t^{\alpha} \tag{4}$$

$$\sigma_t = c\sigma_b t^{\beta} \tag{5}$$

$$t = cd \tag{6}$$

where α and β are the exponents; μ_a and σ_b are intercepts derived from linear regression of $\log(\mu_t)$ and $\log(\sigma_t)$ versus $\log(t)$ for parameters spanning durations $d \geq 24$ h; and c (dimensionless) is an adjustment for sub-daily rainfall intermittency. Parameters α, β, μ_a and σ_b were obtained from observed and downscaled daily rainfall series for each city; the correction c was set to 0.333 based on the median number of hours (8) with non-zero rainfall during the 20 days with largest 24 h totals at the Kanyanya AWS (Tables S3 and S4). This value was confirmed by sensitivity testing and by reference to another site in the tropics (Dunkerley 2019). We used separate terms for each Gumbel parameter to maximise flexibility of scaling across different durations and climatic regimes. Lastly, sub-daily extreme rainfalls were estimated using:

$$I_{t,T} = \mu_t - \sigma_t \ln\left\{-\ln\left(1 - \frac{1}{T}\right)\right\} \tag{7}$$

where $I_{t,T}$ is the maximum rainfall intensity (mm/h) for durations $t \leq 24$ h and return period T (years).

(a)

(b)

(c)
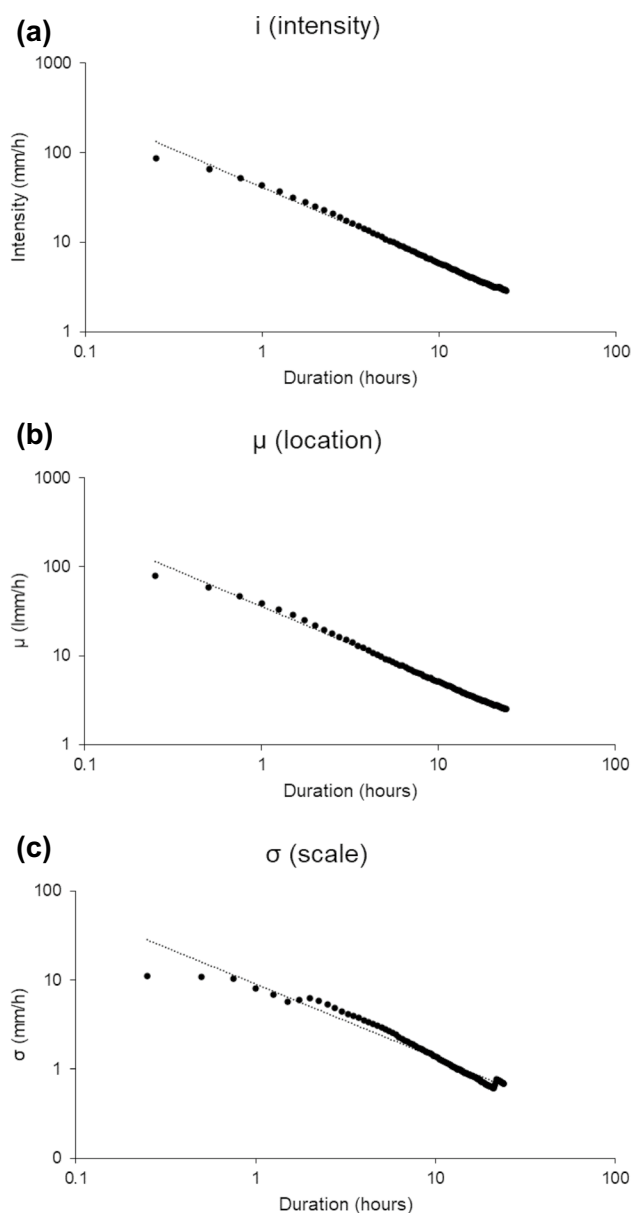
Fig. 4 Scaling of sub-daily AWS **a** intensity, Gumbel **b** location and **c** scale parameters with duration at Kanyanya, Kampala based on 15 min AWS observations during 2017–2021

3.3 Step 3: temporal scaling of sub-daily extreme rainfalls under climate change

Having evaluated temporal scaling of sub-daily extreme rainfalls under the present climate, we explore the sensitivity of IDF tables to (a) RCM with or without convection permitting schemes; (b) temporal scaling method (moments or parameters); and (c) upper bound days for temporal scaling (d_u). Since the future IDF table is unknown, we attempt to emulate changed extreme rainfalls in CP4 and P25 using the two temporal scaling methods. In this way, we evaluate

the ability of each at reproducing the changed climate IDF tables as if the changed climate RCM extreme rainfalls are truth—a test first devised by Charles et al. (1999) to validate the transferability of calibrated statistical downscaling methods between present and future climate conditions.

To denote the various RCM-temporal downscaling combinations we apply the following notation for IDF tables estimated in the following three ways (from CP4 output): (1) directly from RCM bias corrected maxima (CP4); (2) RCM scaled by moments (CP4m); and (3) RCM scaled by parameters (CP4p). The notations for P25 for the same permutations are: P25; P25m; and P25p. Likewise, for SDSM they are: SDSM, SDSMm, and SDSMp.

4 Results

4.1 Predictor suites for heavy rainfall and flooding

SDSM was calibrated with daily precipitation observations and NCEP predictors for the period 1993–2015, setting the wet-day threshold as ≥ 1 mm to exclude trace rainfalls, and the ensemble size to 20. The simplest approach to downscaling local rainfall is to deploy NCEP precipitation as the sole predictor variable (suite P). Previous studies show that methods using precipitation as a predictor can outperform suites comprised of conventional predictors such as atmospheric thickness and humidity (Widmann et al. 2003; González-Rojí et al. 2019). Figure 5 and Fig. S3 show that downscaling NCEP precipitation yields a good match for monthly wet-day occurrence and rainfall totals but there is a tendency to underestimate maximum 1- and 2-day rainfall totals in some of the most extreme months, especially for Kisumu (Table 3).

SDSM was also calibrated on the basis of the correlation matrix, partial correlation matrix, and amount of variance explained by different combinations of predictors. This semi-objective procedure yielded a second predictor suite (C) comprised of three variables: LFTX, PWTR and H850. The predictor set marginally improves simulations of the maximum 1- and 2-day rainfall totals (Table 3).

Predictor variable selection may be informed by other criteria. There were 41 media reports of flooding in Kampala during 2000–2016 and 21 in Kisumu during 2003–2016 (Tables S1 and S2). This equates to mean annual frequencies of ~ 2.5 and ~ 1.5 events per year, respectively, that were sufficiently impactful to be newsworthy. Coincident station records for Kampala suggest that most events were associated with rainfalls on the same or previous day totalling ~ 20 mm. However, the data also show that 24 h rainfall totals of this magnitude occur on average 22 times per year. The equivalent threshold rainfall for media reports of flooding in Kisumu was also ~ 20 mm, which occurs on average
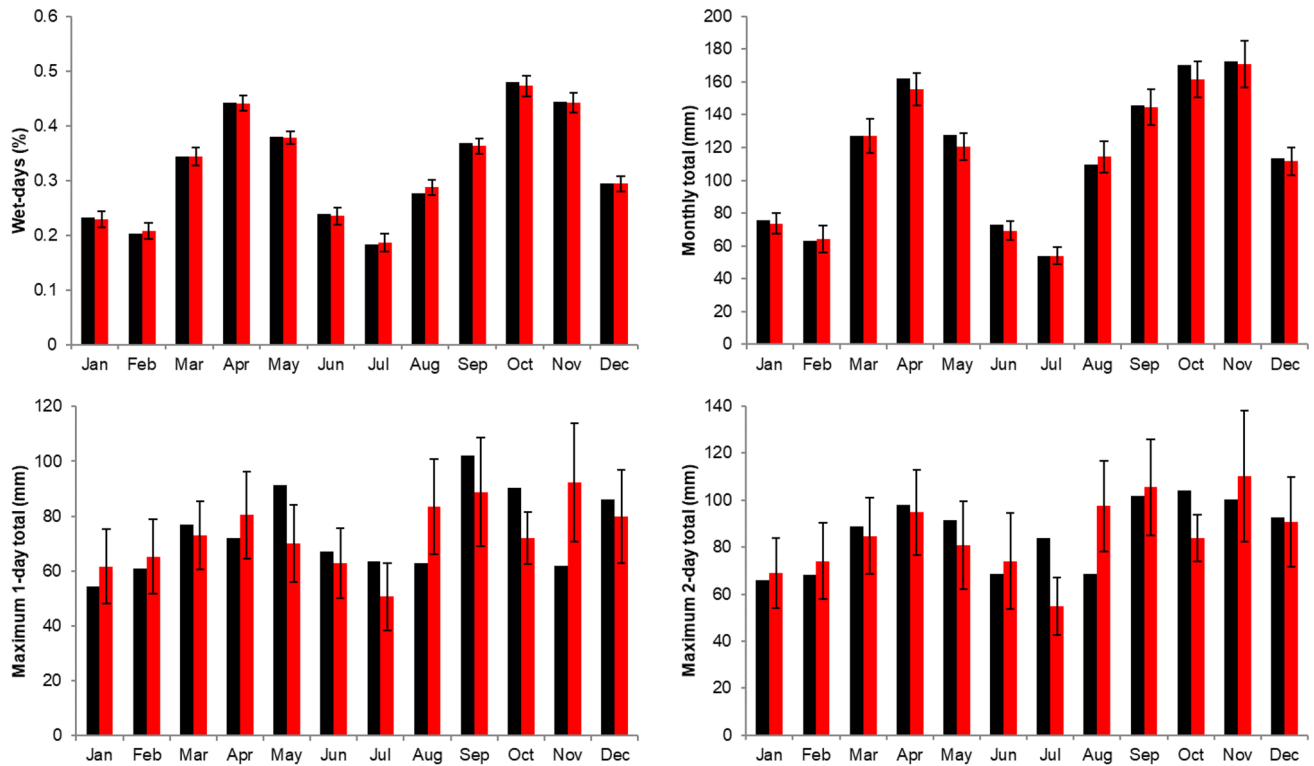
Fig. 5 Observed (black) and SDSM (red) daily precipitation diagnostics for Kampala 1993–2015 produced by predictor suite P. T-bars denote the standard deviation of the SDSM ensemble. The wet-day threshold is 1 mm

Table 3 Mean Absolute Errors (%) in six diagnostics of downscaled daily rainfall by predictor variable suite (P, C and F) for Kampala and Kisumu during the period 1993–2015, based on mean monthly values

| Predictor suites	Wet-day frequency	Wet-day mean	Wet-day variance	Monthly totals	1-day maxima	2-day maxima
Kampala						
P	3	2	21	2	25	22
C	1	2	20	2	16	10
F	1	2	20	2	17	12
Kisumu						
P	1	2	24	2	20	24
C	2	3	25	3	18	21
F	1	3	26	3	18	22

20 times per year. About 65% of these events occur during either the long (March–May) or short (October–December) rains.

These results may reveal that flooding is so commonplace in both cities as to be newsworthy only in the most extreme cases (such as loss of life) and that more frequent, 'nuisance' events are seldom reported. Alternatively, local meteorological records may not fully reflect catchment-wide variations in the amount and timing of heavy rainfall. Other factors could also be contributing to flood severity, such as whether urban drainage systems are waterlogged or blocked. Our scraping of media for flood stories may have overlooked

some events too, but this possibility was minimised by triangulating across multiple sources.

With these issues in mind, dates of newspaper reports or very heavy rainfall (> 50 mm) in Kampala were used to sub-sample NCEP daily downscaling predictor variables. Mean predictor values for the day before and on the day of a flood (or heavy rainfall) were then compared with all other days in the corresponding sampling period. Compositing data in this way reveals that mean DSWR, PWTR, R500, R850 and RHUM have opposite signs on days with and without reported flooding (Fig. 6a); likewise for PWTR, R500, R850 and RHUM on days with/

Fig. 6 Normalized downscaling predictor variables on **a** days before or during a reported flood in Kampala compared with all days in the period 2000–2015; **b** days before or with heavy rainfall (> 50 mm) in Kampala compared with all days in the period 2000–2015. Note that values for NCEP precipitation [PREC] are scaled by 0.1 and are in units mm/d
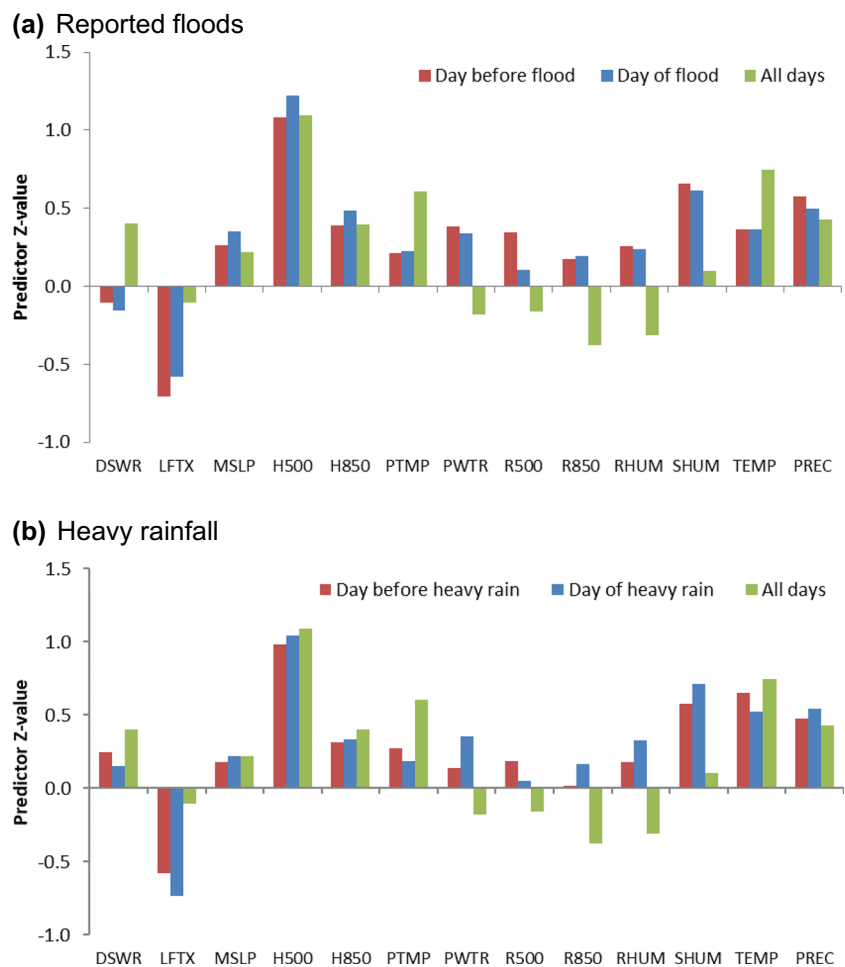
without heavy rainfall (Fig. 6b). Overall, LFTX, SHUM and RHUM have the largest absolute differences in predictor values between the two samples. When considering covariance amongst predictors, the suite (F) with highest partial correlations reduces to PTMP, PWTR, RHUM and R500 (Table 2). The emphasis attached to humidity variables is consistent with previous analyses of moisture flux and heavy rainfall over the region (Finney et al. 2020b).

Use of these predictors in downscaling suite F explicitly captures the regional atmospheric conditions associated with flood-generating rainfalls. However, the gain in downscaling skill is modest. At both sites, predictor suites C and F yield lower Mean Absolute Errors (MAEs) than suite P for the 1- and 2-day monthly maxima (Table 3). Across the three predictor suites, the MAE of the 1-day monthly maxima is 16–25% for Kampala and 18–20% for Kisumu; the MAE ranges for 2-day mean monthly maxima are 10–22% and 21–24%, respectively. Biases in the 1- and 2-day maxima are of interest because they are propagated by the methods of sub-daily scaling below.

4.2 Spatial downscaling daily rainfall totals and annual maximum series

Annual maximum series of daily rainfall totals were extracted from the downscaled predictor suites, then each fit to the Gumbel distribution (Fig. 7). These provide more reliable indications of downscaling skill than individual maxima in each month (above). When distributions of observed and downscaled maxima are compared, the MAE for Kampala was 2.0 mm, 2.7 mm and 2.8 mm for suites P, C and F, respectively. Equivalent MAEs for Kisumu were larger (14.7 mm, 13.0 mm and 12.0 mm, respectively), however, as noted before, there is low confidence in some extreme values at this site. Overall, maximum errors equate to rainfall intensities ~0.5 mm/h regardless of the predictor suite or site. Therefore, on the basis of parsimony, predictor suite P was carried forward into the remaining analyses (although it is acknowledged that suite F is marginally best for Kisumu).

Annual maximum daily rainfall totals and the frequency of days exceeding specified thresholds (20, 30, 40, 50, and
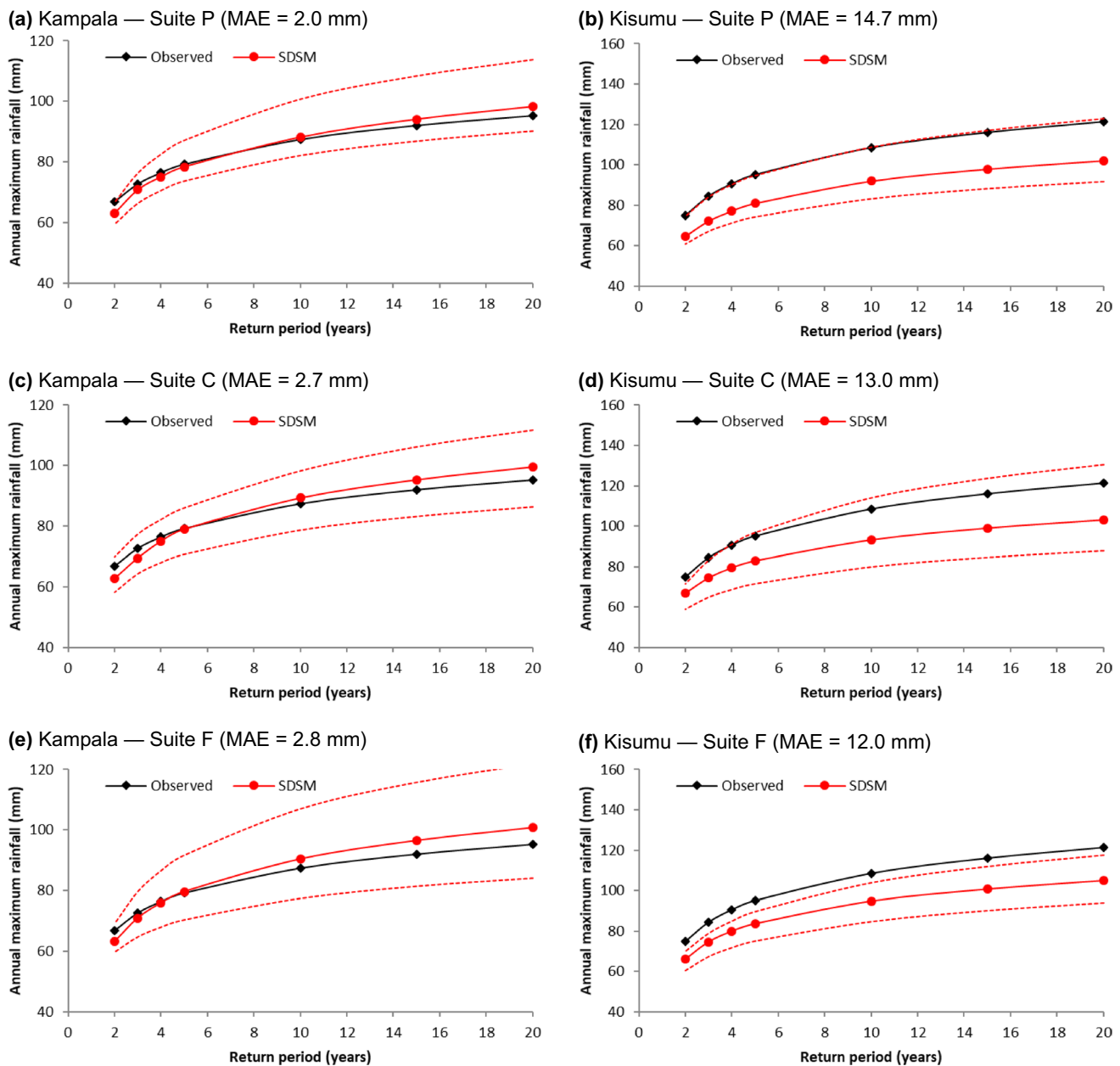
Fig. 7 Effect of downscaling predictor **a**, **b** suite P, **c**, **d** suite C, and **e**, **f** suite F on Gumbel estimates of annual maximum 24 h rainfall totals compared with observations in Kampala (left) and Kisumu (right). Dashed lines are the 95% confidence intervals of the SDSM ensemble range

60 mm/d) exhibit considerable inter-annual variability in both observed and downscaled series (Fig. 8). Trends in these series are all statistically insignificant (p > 0.05), suggesting that the extreme values are stationary in both the observed (1993–2015) and downscaled (1948–2015) series. According to the *t*-test there is no significant difference (p > 0.05) between mean annual frequencies of flood-generating rainfalls in observed and downscaled series for Kisumu. The 20 mm threshold was exceeded on average 20.6 and 19.0 times per year during 1993–2015 in observed and downscaled series, respectively. Equivalent frequencies

of rainfalls exceeding 20 mm in Kampala were 22.3 and 20.8 and are likewise statistically indistinguishable (p > 0.05). Overall, downscaling under-estimates the frequency of flood-generating rainfalls.

4.3 Temporal scaling sub-daily extreme rainfalls (present climate)

Temporal scaling of sub-daily extreme rainfall is feasible because intensities and (Gumbel) distribution parameters (σ, μ) vary with duration (Menabde et al. 1999). Temporal
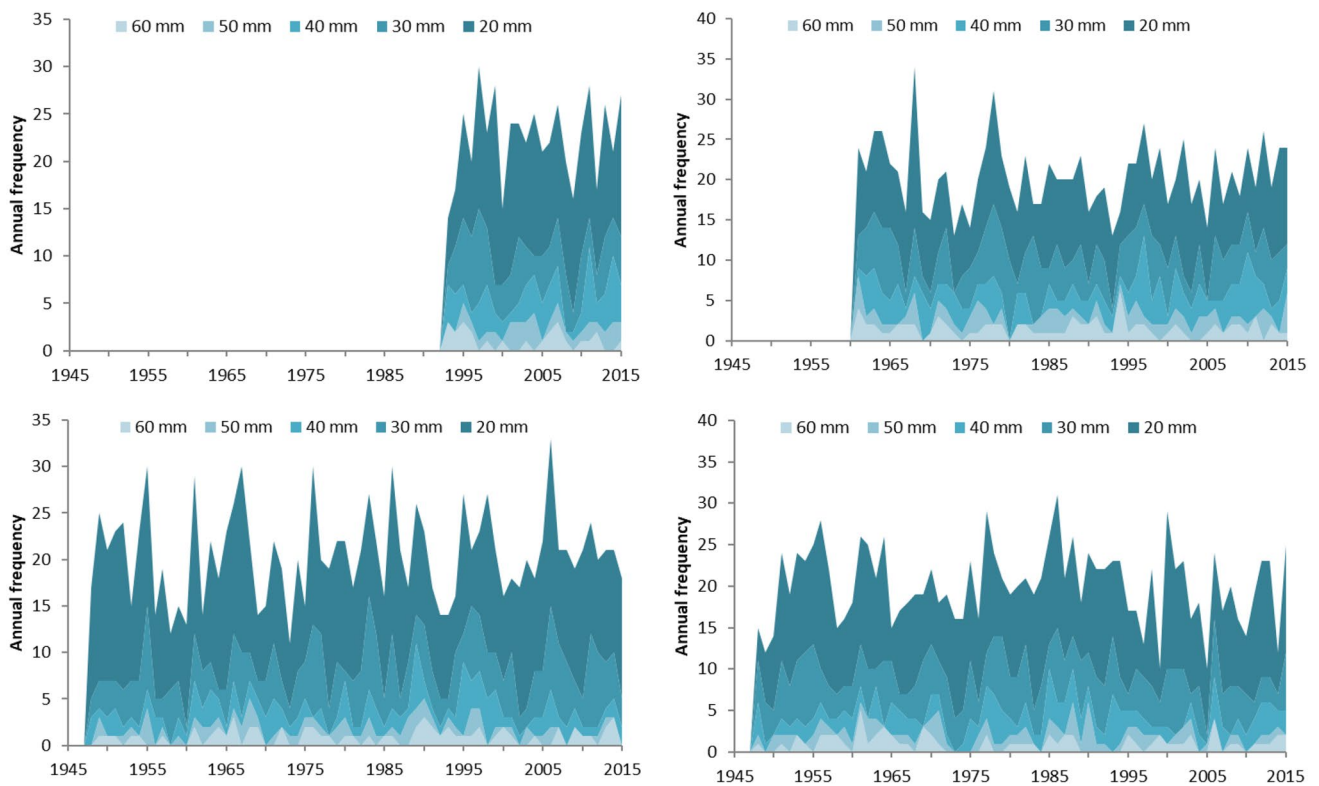
Fig. 8 Observed (upper panels) and SDSM reconstruction (lower panels) of heavy rainfall frequencies for daily total exceeding given thresholds in Kampala (left) and Kisumu (right)
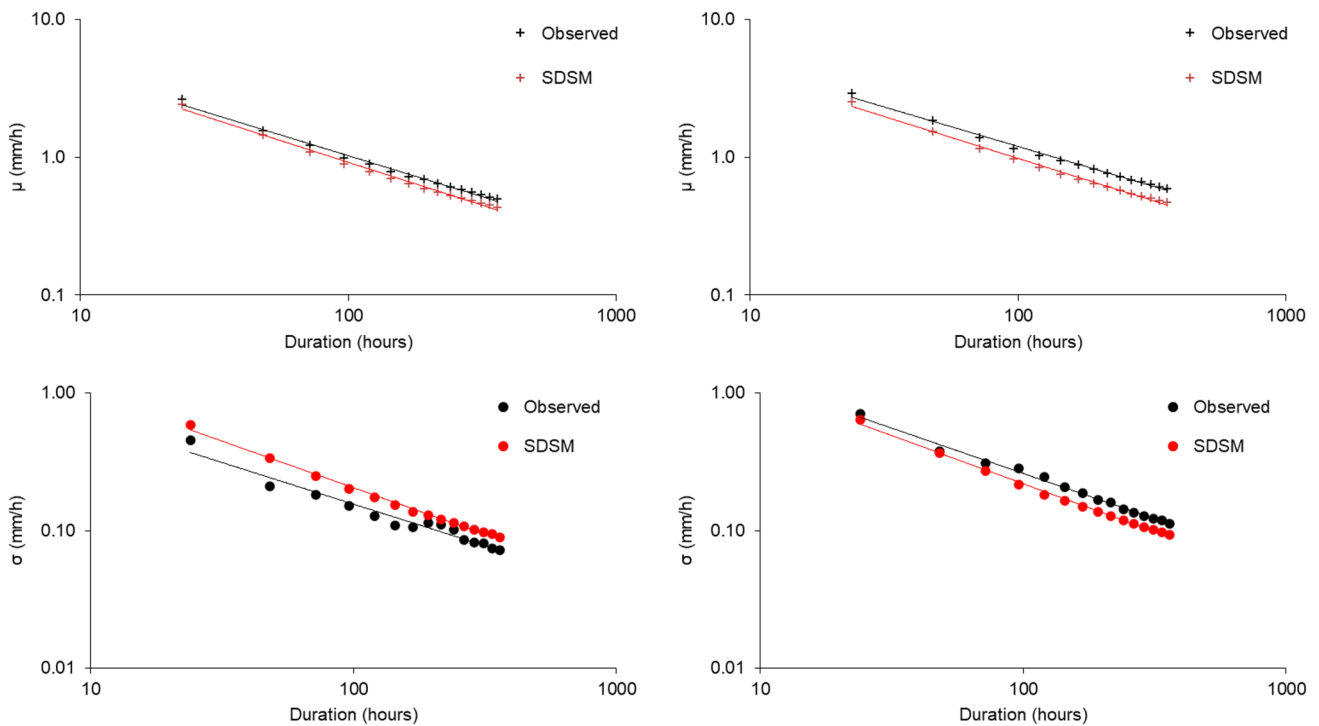
Fig. 9 Gumbel parameters (μ, σ) based on observed and SDSM annual maximum series of rainfall over d = 1–15 days for Kampala (left) and Kisumu (right) during 1993–2015

Table 4 Mean Absolute Errors (%) when temporal and spatial downscaling sub-daily extreme rainfall for Kampala and Kisumu over durations 1, 3 and 6 h, with return periods 2, 5, 10 and 20 years

	Kampala (%)		Kisumu (%)	
	$d_u = 2$	$d_u = 4$	$d_u = 2$	$d_u = 4$
AWS	10	10	–	–
AWSm	19 (10)	31 (23)	–	–
AWSp	18 (12)	22 (17)	–	–
OBSm	27	42	36	48
OBSp	5	20	13	21
NCEP-SDSMm	34	39	38	41
NCEP-SDSMp	14	18	18	19
P25*	34	34	46	46
P25m*	50	53	59	63
P25p*	25	28	51	40
P25-SDSMm	29	36	35	40
P25-SDSMp	43	19	46	19
CP4*	45	45	45	45
CP4m*	71	63	48	54
CP4p*	45	62	21	44
CP4-SDSMm	32	37	42	45
CP4-SDSMp	38	17	27	22

All error estimates are given with respect to T&L; values in brackets for Kampala are when compared with AWS instead of T&L. OBS are observations of daily rainfall manually recorded by UNMA and KMD at Kampala and Kisumu respectively. Models* are bias corrected

scaling is evident in observed and downscaled Gumbel parameters for rainfall durations spanning 24–360 h in both Kampala and Kisumu (Fig. 9). However, there are differences between observed and downscaled parameters: SDSM underestimates both parameters except for σ in Kampala. Whereas the gradient of the scaling relationship for μ is generally stable over the range of time analysed, this is less so for σ. For instance, in Kampala, sub-daily estimates of observed σ would be markedly different if extrapolating from the gradient between 48 and 24 h compared with the slope between 72 and 24 h. These subtle variations confirm the potential sensitivity of σ and μ estimates to the specified upper-bound scaling duration, d_u. Model parameters are given in Tables S3 and S4.

In the absence of multi-decadal sub-daily rainfall records, we evaluated the two temporal scaling methods and sensitivity of errors to d_u using the T&L IDF tables for Kampala and Kisumu, supplemented by evidence from the 15-min AWS data for Kampala (Table 4). The MAE (%) was calculated for each model with respect to observed and estimated extreme rainfalls using IDF tables of 1, 3 and 6 h duration, each with return periods of 2, 5, 10 and 20 years. Throughout, it was assumed that the IDF tables provided by T&L were still valid for climate conditions in

1993–2015. The previously mentioned trend analysis for SDSM peaks over threshold supports this view.

Table 4 shows that the MAE for the 5-year AWS record was 10% when compared with T&L. This can be regarded as the aggregate uncertainty reflecting climate variability, the brevity of the record, and differences between sites in Kampala. Temporal scaling of daily observations (OBSp) for Kampala by the method of parameters ($d_u = 2$) has an MAE (5%) that lies within this uncertainty bound. However, the MAE for all other temporally scaled observations ranges between 13 and 48%. Across both sites and both d_u, the average MAE is 43% for the method of moments, and 28% for the method of parameters. Regardless of temporal scaling method (or none for CP4 and P25) the average MAE is 31% for SDSM, 44% for CP4, and 49% for P25. Overall, the best spatial–temporal downscaling model combination was the method of parameters applied to NCEP-SDSM (MAE = 14%); the worst combination was the method of moments applied in CP4m (MAE = 71%). MAE were on average marginally lower for Kampala (38%) than Kisumu (40%); they were also lower on average for $d_u = 2$ (38%) than $d_u = 4$ (40%).

MAEs for the IDF table as a whole conceals variations in skill between temporal and spatial downscaling methods at different durations and return periods. Figure 10 shows estimated extreme rainfalls over 1, 3 and 6 h for Kampala and Kisumu, using observed and downscaled annual daily maxima as input to the moment and parameter scaling methods. Regardless of input data (observations or SDSM), duration, or return period, errors are always smaller when temporal scaling by the method of parameters (rather than moments). For example, the error in maximum 3 h intensity with 20 year return period (henceforth 3D20T) produced by SDSMp was 12% for Kampala, and 16% for Kisumu (compared, respectively with 33% and 38% for SDSMm). Overall, the smallest error (6%) in 3D20T was produced by UNMAp for Kampala, supporting the view that daily records can be used to estimate sub-daily extreme rainfalls (at this site) to within measurement error. So far, the most extreme storm recorded by the AWS network in Kampala had peak intensity of ~ 140 mm/h for 15 min and ~ 75 mm/h for 1 h which equates to a 20-year event (1D20T) in the T&L table (given as 73 mm/h). A comparable 1D20T rainfall intensity (77 mm/h) was scaled by UNAMp from daily data. Similar, 1 h maxima are reported for sites in Rwanda (Demarée and Vyver, 2013) and Tanzania (De Paola et al. 2014).

Visual inspection of 15-min data for Kampala suggests *multi-scaling* as seen by breaks in the gradient of the intensity-duration relationship (Fig. 4a). Discontinuities occur in the maximum intensity at durations less than 1 h, and for the parameter scaling around 2 h (Fig. 4b and c). Below the 1 h threshold, temporal scaling tends to over-estimate rainfall intensities. Similarly, a 1 h break-point has been reported
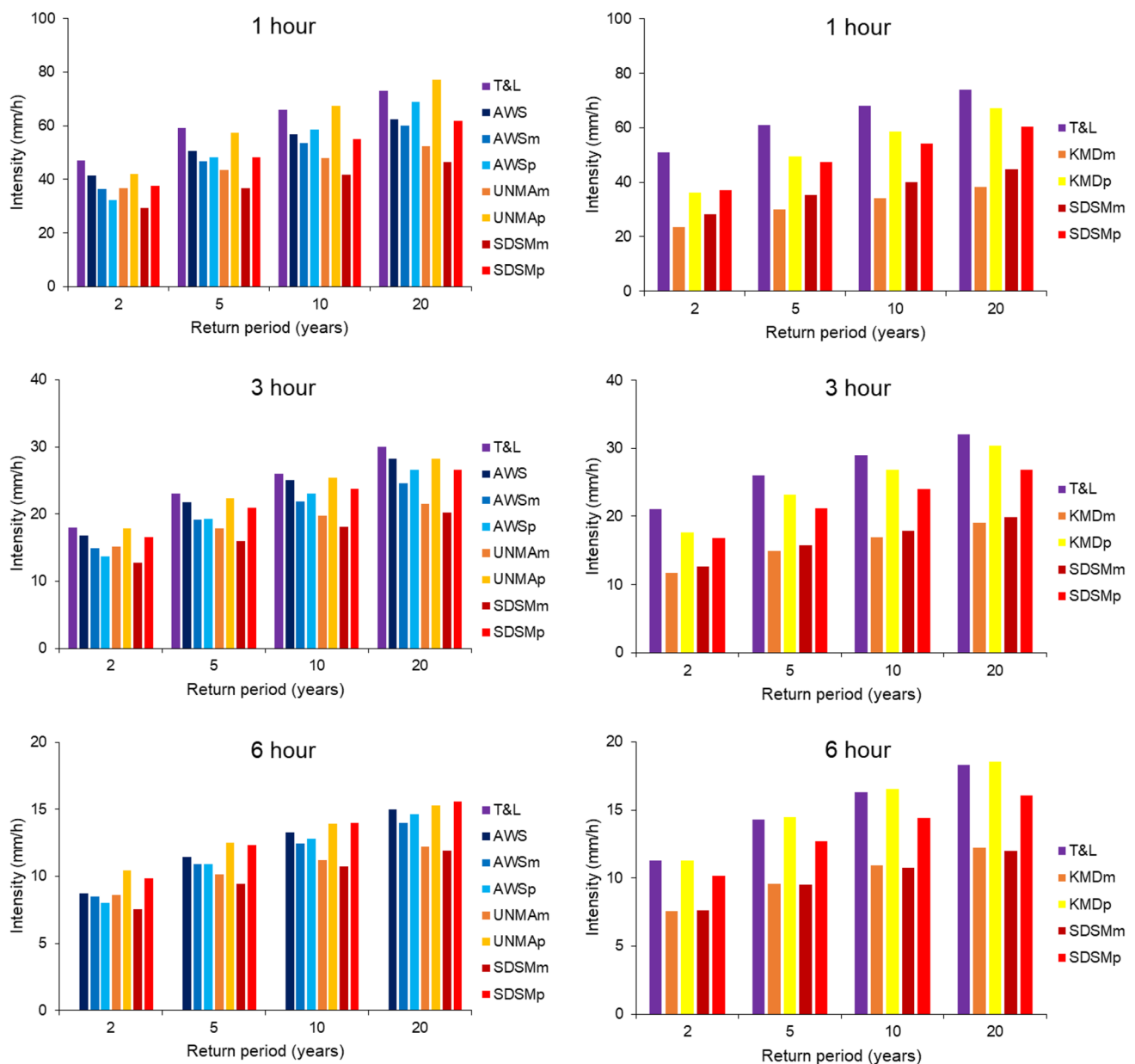
Fig. 10 Sub-daily IDF estimates for Kampala (left) and Kisumu (right). Observed extreme rainfalls were based on the T&L 15-min tables for 1931–1954 (noting that no 6 h extreme values are given for Kampala) and 15-min record at Kanyanya (AWS). Other estimates were based on moments (m) and parameters (p) scaled from annual maximum 1- and 2-day ($d_u = 2$) rainfall series from AWS, observed (UNMA, KMD), or downscaling (SDSM)

for IDF curves elsewhere in the tropics (Demarée et al. 2013; Kuok et al. 2016), and at 3 h globally (Courty et al. 2019). On the balance of evidence, we caution that temporal scaling from observed daily data is unreliable for extreme rainfalls with durations less than 1 h at Kampala and Kisumu.

4.4 Temporal scaling sub-daily extreme rainfalls (changed climate)

The two temporal scaling methods were applied to RCM annual maximum daily and multi-day rainfall series to determine how well they recover sub-daily extreme rainfalls simulated by the same RCMs under changed climate

Table 5 MAE (%) in IDF tables estimated by temporal (moment, parameter) scaling of P25 and CP4 compared with unscaled P25 and CP4 output under future climate forcing for upper scaling period $d_u = 2$ and $d_u = 4$ days

	Kampala (%)		Kisumu (%)	
	$d_u = 2$	$d_u = 4$	$d_u = 2$	$d_u = 4$
P25m	28	27	76	42
P25p	29	26	133	22
CP4m	54	36	40	36
CP4p	164	15	30	9

forcing (here for illustrative purposes, RCP8.5). As before, we compared model variants using the MAE for IDF tables comprised of maximum 1-, 3-, and 6-h rainfall intensities, with 2, 5, 10 and 20 year return periods. We most closely examined extreme rainfalls with 20-year return periods given their relevance to pluvial flooding. This event severity is comparable to the design standard used by Kampala Capital City Authority for primary and secondary drains with no freeboard.

As shown previously, spatial and temporal scaling generally reduces errors in unscaled sub-daily output from CP4 and P25 for the present climate (Table 4). For Kampala, without scaling, the overall MAE was 45% for CP4 and 34% for P25; with hybrid (RCM-SDSM) scaling these were 19% for P25-SDSMp ($d_u = 4$) and 17% for CP4-SDSMp ($d_u = 4$). Equivalent gains in accuracy for Kisumu were from 45% (CP4) and 46% (P25) to 22% (CP4-SDSMp) and 19% (P25-SDSMp), respectively. Hence, SDSM (with scaling by parameters) significantly improved the accuracy of sub-daily extreme rainfalls produced by CP4 and P25 for both cities, under the present climate.

When scaled daily extremes in an RCM are used to estimate sub-daily extreme rainfalls in the same RCM, smallest errors are again produced by parameter scaling (Table 5). For Kampala, the MAE were 15% (CP4p) and 26% (P25p), compared with 36% (CP4m) and 27% (P25m). For Kisumu, the MAE were 9% (CP4p) and 22% (P25p), compared with 36% (CP4m) and 42% (P25m). The supports the view that under a changed climate scenario, temporal scaling by the method of parameters yields smaller errors than the method of moments, and that these errors are lowest overall for the higher resolution RCM with convection-permitting scheme (i.e., CP4p). Moreover, these errors are lower for $d_u = 4$ than $d_u = 2$.

Unscaled RCM simulations project changes in 3D20T of $+7\%$ (P25) to $+82\%$ (CP4) in Kampala, and $+38\%$ (CP4) to $+259\%$ (P25) in Kisumu. Scaling RCM simulations by the method of parameters yields 3D20T of similar order: in Kampala they are $+59\%$ (P25p) to $+173\%$ (CP4p), and in Kisumu $+20\%$ (CP4p) to $+228\%$ (P25p). Equivalent

changes in 3D20T when scaling by the method of moments are $+52\%$ (P25m) to $+202\%$ (CP4m) for Kampala, and $+9\%$ (CP4m) to $+430\%$ (P25m) for Kisumu. Hence, the method of moments tends to give larger upper bound estimates of 3D20T than unscaled RCM simulations, as well as the method of parameters.

The projected increases in both unscaled and scaled CP4 and P25 extreme rainfall likely exceed Clausius-Clapeyron rates. There can be physical reasons for this, such as enhanced updraft velocity driven by increased latent heat release from condensation (Pfahl et al. 2017). However, it is also likely to reflect the combined influence of climate variability/short (10 year) simulation periods, and large variations in rainfall metrics between neighbouring model grid cells (not shown). The RCM experiments used herein project 10–15% fewer hours with rainfall and 14–31% shorter wet-spells—conditions resulting in average rainfall intensities that are 6–72% heavier.

Preliminary analysis of CP4 intensities (for Kampala) reveals that present and changed climate simulations exhibit power-scaling of unscaled rainfall intensities (Fig. S4) as seen in observations (Fig. 4a). Like observations, a break-point is evident at shortest durations, signalling multi-scaling and suggestive of limits to growth of intensities at durations less than ~ 3 h. The break in slope also denotes the point at which errors expand when temporal scaling from daily RCM output to sub-daily extreme rainfalls. Until this can be confirmed for other RCMs, 3 h is recommended as the finest temporal resolution at which extreme rainfall can be scaled from RCM annual maximum series of daily rainfall.

5 Discussion

Spatial downscaling was performed using SDSM with three predictor suites to generate multi-decadal, daily rainfall series for Kampala and Kisumu. These daily simulations were then used to build multi-day annual maximum rainfall series, from which sub-daily scaling relationships could be established for the parameters of an extreme value distribution (Gumbel). We demonstrated that temporal scaling of the extreme value distribution parameters—rather than by the method of moments—yields superior results under present and changed climate conditions (as simulated by RCMs). Our three-step workflow is intended to be transferrable to other cities and complex environments (such as small islands or mountainous regions) where knowledge of extreme rainfall hazards is urgently needed, yet such data may be difficult to source. However, the transferability of the approach rests on several practical considerations.

First, we assumed that simple- rather than multi-scaling applies across a defined range of durations. In other words,

extreme rainfall is treated as a continuum of processes operating over sub-daily to multi-day scales. Whether short- or long-duration events, heavy rainfall in the LVB is associated with organized patterns of convection and, for Kampala, simple-scaling appears to hold over durations from about 1–96 h. Tapering of the rate of increase of intensities at durations less than 1 h probably reflects physical limits to rain-drop size, atmospheric moisture content and updraft speeds. Levelling of intensities over durations longer than 96 h may be due to a greater proportion of time as dry interludes. However, understanding of present and future drivers of extreme rainfall in the vicinity of Lake Victoria is still evolving (Chamberlain et al. 2014; Thiery et al. 2015, 2016; Finney et al. 2019; 2020a). Satellite observations reveal a marked diurnal cycle of thunderstorm activity that peaks over surrounding land in late afternoon and above the lake during the night, linked to switches in convection and moisture advection. Heavy rainfall over multiple days may be associated with large stationary/sequential disturbances but the synoptic systems favouring such conditions in the LVB are poorly understood. Beyond the LVB, the range of simple-scaling may be bounded by different durations (Courty et al. 2019).

Second, conventional methods treat sub-daily and daily intensities in the same way by assuming that rain falls at a uniform rate throughout the whole duration. In reality, single- and multi-day periods comprise mixtures of wet- and dry-spells. Nearly half of all days with non-zero rainfall recorded by the AWS in Kampala, were actually raining for only 3 h or less (i.e., dry for 21 h in the day). As a first approximation, daily totals could therefore be viewed as equivalent to 3 h rainfall totals. Indeed, the T&L estimate of 3D20T for Kampala is 90 mm, whereas our 20-year observed 24 h estimate is 96 mm. Likewise, for Kisumu the 3D20T and 24 h estimates are 96 mm and 120 mm, respectively. As the median time with rainfall during the 20 most extreme rainfall events recorded by the AWS was ~8 h, we specified the correction factor for rainfall intermittency as $c = 0.333$. However, this factor will be site specific and could be discerned from short field campaigns, sub-daily re-analyses, or satellite data.

Third, the rainfall series used to calibrate the spatial and temporal downscaling methods are assumed to be accurate and homogenous, despite possible changes in measurement practices, instrumentation, site (properties) and/or external forcing. For instance, the $0.1° \times 0.1°$ gridded African Rainfall Climatology version 2 suggests that there has been a long-term decline in *average* daily rainfall over Uganda during the last 34 years (Ssentongo et al. 2018; Ongoma et al. 2018). Although the observed annual daily maxima for Kampala and Kisumu are stationary, further work is needed to determine whether coherent trends are emerging in extreme rainfall across other parts of the LVB. Doubt

remains about the provenance of some extreme daily totals in the Kisumu record, and these uncertainties are carried into the spatial and temporal scaling relationships.

Fourth, we applied the Gumbel distribution for comparability with previous work in the region (T&L) and for parsimony. However, others favour the GEV (Nguyen et al. 1998; Herath et al. 2016; Lima et al. 2016, 2018; Courty et al. 2019), log-Pearson type III (Kuok et al. 2016; Olofintoye et al. 2009), generalized Pareto distribution (Kristvik et al. 2019), or four-parameter beta distribution (Lima et al. 2016). Each could yield different rainfall estimates depending on the site-specific suitability of the distribution and uncertainty in parameter estimates. Some studies use stochastic weather generators to disaggregate and adjust synthetic rainfall series for climate change (Shrestha et al. 2017; So et al. 2017). Choices about downscaling method (Wilby et al. 1998), re-analysis product (Manzanas et al. 2015), baseline period (Fadhel et al. 2017), climate model and emissions scenarios (Alam and Elshorbagy 2015) also affect simulations of extreme rainfall. Given that it would be impractical to represent all these elements in resource-constrained situations, justification and transparency of all methodological decisions is essential.

Fifth, we tested the sensitivity of extreme rainfall estimates to the upper-bound scaling duration ($d_u = 48$ h or 96 h). As with the correction factor for rainfall intermittency (c), the optimal value of d_u will depend on local rainfall mechanisms. For example, at Kisumu, a break-point in σ scaling above 96 h may reflect a shift between weather regimes producing persistent heavy rainfall (Fig. 9). Again, even a few seasons of sub-hourly rainfall observations could help to identify such break-points or multiscaling at data sparse sites to inform the choice of d_u.

Our main objective was to test the robustness of two temporal scaling methods under present and changed climate conditions. Results for Kampala and Kisumu show that the method of parameters yields reliable 3- and 6-h extreme rainfalls for the present climate when compared with historic IDF tables and available AWS records. The parameter scaling method also achieved MAEs of 9–26% (compared with 27–42% by moments) when scaling IDF tables under changed climate conditions (see Table 5). However, we do recognise that alternative scaling techniques are available. For instance, others have implemented Bayesian frameworks to condition the location parameter of the GEV distribution on historic rainfall with non-stationary extremes (Cheng and AghaKouchak 2014; Lima et al. 2016, 2018; Tfwala et al. 2017), or have uniformly adjusted IDF tables with the same 'delta' applied across all return periods and durations to capture climate change (Kuok et al. 2016). The robustness of these methods under climate change could also be tested within RCM 'worlds' as herein.

Finally, we presented a new method for guiding downscaling predictor variable selection based on their covariance with newsworthy flood episodes. Although this did not always result in more skilful downscaling, the identification of impactful rainfall thresholds enables our results to be communicated with greater relevance. For example, under the illustrative CP4 scenario, Kampala could see exceedances of the critical 20 mm event increase by 10–12 days per year by ~ 2100, compared with 20 events per year presently. Without improvements in urban drainage systems and development control, these would translate into more frequent surface water floods. Future research could explore the use of social media and crowdsourced flood information to stratify downscaling predictors and extreme rainfall events (Wang et al. 2018; Thompson et al. 2022). With longer and more accurate media records, it may be possible to develop more skilful downscaling of extreme rainfall linked to flood-generating episodes. Multi-media sources could also be used to analyse the detailed evolution and socio-economic impacts of individual flash flood events in Kampala.

6 Conclusions

IDF tables are widely used in water infrastructure design and management. Therefore, they are a useful entry point for bringing adjustments for climate change into engineering practice. To date, there have been very few studies of climate change impacts on cities in tropical regions. We added to this knowledge base by: analysing concurrent rainfall and media reports to determine critical thresholds of rainfall and infer downscaling predictors relevant to pluvial flooding; using daily rainfall records to calibrate spatial and temporal scaling models of sub-daily extreme rainfalls for sites in the tropics; and evaluating the robustness of two temporal scaling methods *within* RCM simulations of climate change.

Four new methodological insights emerged from our research. First, that media reports (of pluvial flooding) can be used to guide downscaling model calibration and to specify meaningful thresholds of impactful rainfall—in this case ~ 20 mm in a day is sufficient to cause reportable flooding in either city. Second, the lesser known method of parameter scaling yields smaller errors in extreme rainfalls (IDF tables) than the more widely adopted method of moments—a finding that applies to scaling from observations, and downscaling by NCEP-SDSM, RCM (P25, CP4), and hybrid (CP4-SDSM, P25-SDSM) methods. Third, temporal scaling is sensitive to sub-daily rainfall intermittency (c) and the upper-bound duration (d_u) used to scale the extreme value distribution parameter—here specified as $c = 0.333$ of a day, and $d_u = 4$ days for optimal scaling of extreme rainfalls. Fourth, there are lower errors in IDF tables when scaling RCM simulations of the changed climate by the method of parameters—especially when scaling rainfall from the convection-permitting RCM (CP4). This increases confidence in the accuracy of spatially and temporally downscaled extreme rainfalls under changed climate conditions.

Further research is needed to assess the sensitivity of downscaled IDF tables to other methodological details. These include the source(s) and set(s) of predictors used to calibrate the statistical downscaling model; the distribution and parameters describing sub-daily extreme rainfalls; sampling uncertainty and non-stationarity in these parameters; and choice and resolution of RCM(s). Ultimately, any projections of future extreme rainfalls will depend on the realism of the climate model over the study area. Convection-permitting RCMs (with explicit representation of the African Great Lakes) improve confidence in the physical plausibility of proposed adjustments to IDF tables used for designing water infrastructure. Even so, we show the extent to which RCM-statistical downscaling with temporal scaling can improve estimates of sub-daily extreme rainfalls, at least for present climate conditions. Further work is needed to test the skill of these hybrid models under changed climate conditions using carefully designed RCM experiments.

Declarations

Conflict of interest The authors have no relevant financial or non-financial interests to disclose.

References

Agarwal S, Kumar S, Singh UK (2021) Intensity duration frequency curve generation using historical and future downscaled rainfall data. Indian J Ecol 48:275–280

Ahadzie DK, Proverbs DG (2011) Emerging issues in the management of floods in Ghana. Int J Saf Secur Eng 1:182–192

Alam MS, Elshorbagy A (2015) Quantification of the climate change-induced variations in Intensity–Duration–Frequency curves in the Canadian Prairies. J Hydrol 527:990–1005

Ananga EO, Njoh AJ, Adams EA, Peaden C (2019) Factors imped-ing efficient functionality of community operated urban water schemes: the experience of Kisumu, Kenya. Sustain Water Resour Manag 5:1143–1153

Barbosa AE, Fernandes JN, David LM (2012) Key issues for sustain-able urban stormwater management. Water Res 46:6787–6798

Benestad RE, Lutz J, Dyrrdal AV, Haugen JE, Parding KM, Dobler A (2021) Testing a simple formula for calculating approximate inten-sity-duration-frequency curves. Environ Res Lett 16(4):044009

Beranová R, Kyselý J, Hanel M (2018) Characteristics of sub-daily precipitation extremes in observed data and regional climate model simulations. Theoret Appl Climatol 132:515–527

Borges PDA, Barfus K, Weiss H, Bernhofer C (2017) Extended predic-tor screening, application and added value of statistical downscal-ing of a CMIP5 ensemble for single-site projections in Distrito Federal, Brazil. Int J Climatol 37:46–65

Bougadis J, Adamowski K (2006) Scaling model of a rainfall intensity-duration-frequency relationship. Hydrol Process 20:3747–3757

Burlando P, Rosso R (1996) Scaling and muitiscaling models of depth-duration-frequency curves for storm precipitation. J Hydrol 187:45–64

Butcher JB, Zi T, Pickard BR, Job SC, Johnson TE, Groza BA (2021) Efficient statistical approach to develop intensity-duration-fre-quency curves for precipitation and runoff under future climate. Clim Change 164:3

Casas-Castillo MC, Llabrés-Brustenga A, Rius A, Rodríguez-Solà R, Navarro X (2018) A single scaling parameter as a first approxi-mation to describe the rainfall pattern of a place: application on Catalonia. Acta Geophys 66:415–424

Chamberlain JM, Bain CL, Boyd DFA, McCourt K, Butcher T, Palmer S (2014) Forecasting storms over Lake Victoria using a high reso-lution model. Meteorol Appl 21:419–430

Charles SP, Bates BC, Whetton PH, Hughes JP (1999) Validation of downscaling models for changed climate conditions: case study of southwestern Australia. Clim Res 12:1–14

Cheng L, AghaKouchak A (2014) Nonstationary precipitation inten-sity-duration-frequency curves for infrastructure design in a changing climate. Sci Rep 4:7093

City Mayors (2020) The world's fastest growing cities and urban areas from 2006 to 2020. http://www.citymayors.com/statistics/urban_growth1.html. Accessed 15 June 2020

Courty LG, Wilby RL, Hillier J, Slater LJ (2019) Intensity-duration-frequency curves of precipitation at the global scale. Environ Res Lett 14:084045

Crawford T, Betts NL, Favis-Mortlock DT (2007) GCM grid box choice and predictor selection associated with statistical down-scaling of daily precipitation over Northern Ireland. Clim Res 34:145–160

Daly C, Gibson WP, Taylor GH, Doggett MK, Smith JI (2007) Observer bias in daily precipitation measurements at United States Cooperative Network Stations. Bull Am Meteor Soc 88:899–912

de Magny GC, Thiaw W, Kumar V, Manga NM, Diop BM, Gueye L, Kamara M, Roche B, Murtugudde R, Colwell RR (2012) Cholera outbreak in Senegal in 2005: was climate a factor? PLoS ONE 7:e44577

De Paola F, Giugni M, Topa ME, Bucchignani E (2014) Intensity-Duration-Frequency (IDF) rainfall curves, for data series and climate projection in African cities. Springerplus 3:133

Demarée GR, Vyver H (2013) Construction of intensity-duration-frequency (IDF) curves for precipitation with annual maxima data in Rwanda, Central Africa. Adv Geosci 35:1–5

Drakenberg O, Nyangena W, Lokina R (2007) Environmental policy brief for the Lake Victoria Basin. Environmental Economics Unit, Göteborg University

Dunkerley D (2019) How does sub-hourly rainfall intermittency bias the climatology of hourly and daily rainfalls? Examples from arid and wet tropical Australia. Int J Climatol 39:2412–2421

Dunkerley D (2021) Intermittency of rainfall at sub-daily timescales: New quantitative indices based on the number, duration, and sequencing of interruptions to rainfall. Atmos Res 253:105475

Fadhel S, Rico-Ramirez MA, Han D (2017) Uncertainty of Inten-sity–Duration–Frequency (IDF) curves due to varied climate baseline periods. J Hydrol 547:600–612

Finney DL, Marsham JH, Jackson LS, Kendon EJ, Rowell DP, Boor-man PM, Keane RJ, Stratton RA, Senior CA (2019) Implica-tions of improved representation of convection for the East Africa water budget using a convection-permitting model. J Clim 32:2109–2129

Finney DL, Marsham JH, Rowell DP, Kendon EJ, Tucker SO, Strat-ton RA, Jackson LS (2020a) Effects of explicit convection on future projections of mesoscale circulations, rainfall, and rain-fall extremes over Eastern Africa. J Clim 33:2701–2718

Finney DL, Marsham JH, Walker DP, Birch CE, Woodhams BJ, Jack-son LS, Hardy S (2020b) The effect of westerlies on east Afri-can rainfall and the associated role of tropical cyclones and the Madden–Julian oscillation. Q J R Meteorol Soc 146:647–664

Förster K, Thiele LB (2020) Variations in sub-daily precipitation at centennial scale. npj Clim Atmos Sci 3:1–7

Fu G, Charles SP, Chiew FH, Ekström M, Potter NJ (2018) Uncer-tainties of statistical downscaling from predictor selection: equi-finality and transferability. Atmos Res 203:130–140

García-Marín AP, Ayuso-Muñoz JL, Jiménez-Hornero FJ, Estévez J (2013) Selecting the best IDF model by using the multifractal approach. Hydrol Process 27:433–443

González-Rojí SJ, Wilby RL, Sáenz J, Ibarra-Berastegi G (2019) Harmonized evaluation of daily precipitation downscaled using SDSM and WRF+WRFDA models over the Iberian Peninsula. Clim Dyn 53:1413–1433

Gough KV, Yankson PWK, Wilby RL, Amankwaa E, Abarike M, Codjoe S, Griffiths P, Kaba C, Kasei R, Kayaga S (2019) Vul-nerability to extreme weather events in cities: implications for infrastructure and livelihoods. J Br Acad 7:155–181

Gupta VK, Waymire E (1990) Multiscaling properties of spatial rainfall and river flow distributions. J Geophys Res: Atmos 95(D3):1999–2009

Hanel M, Buishand TA (2010) On the value of hourly precipitation extremes in regional climate model simulations. J Hydrol 393:265–273

Hassanzadeh E, Nazemi A, Adamowski J, Nguyen TH, Van-Nguyen VT (2019) Quantile-based downscaling of rainfall extremes: notes on methodological functionality, associated uncertainty and application in practice. Adv Water Resour 131:103371

Haylock MR, Cawley GC, Harpham C, Wilby RL, Goodess CM (2006) Downscaling heavy precipitation over the UK: a comparison of dynamical and statistical methods and their future scenarios. Int J Climatol 26:1397–1415

Herath SM, Sarukkalige PR, Nguyen VTV (2016) A spatial temporal downscaling approach to development of IDF relations for Perth airport region in the context of climate change. Hydrol Sci J 61:2061–2070

Hosseinzadehtalaei P, Tabari H, Willems P (2020) Climate change impact on short-duration extreme precipitation and intensity–duration–frequency curves over Europe. J Hydrol 590:125249

Kalnay E, Kanamitsu M, Kistler R, Collins W, Deaven D, Gandin L, Iredell M, Saha S, White G, Wollen J, Zhu Y, Chelliah M, Ebisuzaki W, Higgins W, Janowiak J, Mo KC, Ropelewski C, Wang J, Leetmaa A, Reynolds R, Jenne R, Joseph D (1996) The NCEP/NCAR 40-year reanalysis project. Bull Am Meteor Soc 77:437–471

Kendon EJ, Stratton RA, Tucker S, Marsham JH, Berthou S, Rowell DP, Senior CA (2019) Enhanced future changes in wet and dry extremes over Africa at convection-permitting scale. Nat Commun 10:1794

Kigobe M, McIntyre N, Wheater H, Chandler R (2011) Multi-site stochastic modelling of daily rainfall in Uganda. Hydrol Sci J 56:17–33

Koutsoyiannis D, Kozonis D, Manetas A (1998) A mathematical framework for studying rainfall intensity-duration-frequency relationships. J Hydrol 206:118–135

Kristvik E, Johannessen BG, Muthanna TM (2019) Temporal downscaling of IDF curves applied to future performance of local stormwater measures. Sustainability 11:1231

Kuok KK, Mah YS, Imteaz MA, Kueh SM (2016) Comparison of future intensity duration frequency curve by considering the impact of climate change: case study for Kuching city. Int J River Basin Manag 14:47–55

Lee T, Park T (2017) Nonparametric temporal downscaling with event-based population generating algorithm for RCM daily precipitation to hourly: Model development and performance evaluation. J Hydrol 547:498–516

Liew SC, Raghavan SV, Liong SY (2014) How to construct future IDF curves, under changing climate, for sites with scarce rainfall records? Hydrol Process 28:3276–3287

Lima CH, Kwon HH, Kim JY (2016) A Bayesian beta distribution model for estimating rainfall IDF curves in a changing climate. J Hydrol 540:744–756

Lima CHR, Kwon HH, Kim JY (2018) A local-regional scaling invariant Bayesian GEV model for estimating rainfall IDF curves in a future climate. J Hydrol 566:73–88

Lu W, Qin X (2020) Integrated framework for assessing climate change impact on extreme rainfall and the urban drainage system. Hydrol Res 51:77–89

Macdonald DMJ, Miller JD, Winterbourn JB, Warnaars TA, Mwebembezi L, Arwat P, Tanywa S (2018) High resolution meteorological data from a network of five stations in Kampala, Uganda. Centre for Environmental Data Analysis. https://doi.org/10.5285/a2a8100c46794985b410ea436f24812a

Manzanas R, Brands S, San-Martin D, Lucero A, Limbo C, Gutiérrez JM (2015) Statistical downscaling in the tropics can be sensitive to reanalysis choice: a case study for precipitation in the Philippines. J Clim 28:4171–4184

Maraun D, Widmann M (2018) Statistical downscaling and bias correction for climate research. Cambridge University Press

Menabde M, Seed A, Pegram G (1999) A simple scaling model for extreme rainfall. Water Resour Res 35:335–339

Nguyen T-H, Nguyen V-T-V (2020) Linking climate change to urban storm drainage system design: an innovative approach to modeling of extreme rainfall processes over different spatial and temporal scales. J Hydro-Environ Res 29:80–95

Nguyen VTV, Nguyen TD, Wang H (1998) Regional estimation of short duration rainfall extremes. Water Sci Technol 37:15–19

Nguyen VTV, Nguyen TD, Cung A (2007) A statistical approach to downscaling of sub-daily extreme rainfall processes for climate-related impact studies in urban areas. Water Sci Technol: Water Supply 7:183–192

Olago D, Marshall M, Wandiga SO, Opondo M, Yanda PZ, Kangalawe R, Githeko A, Downs T, Opere A, Kabumbuli R, Kirumira E (2007) Climatic, socio-economic, and health factors affecting human vulnerability to cholera in the Lake Victoria basin, East Africa. Ambio 36:350–358

Olofintoye OO, Sule BF, Salami AW (2009) Best–fit probability distribution model for peak daily rainfall of selected cities in Nigeria. NY Sci J 2:1–12

Olsson J, Niemczynowicz J, Berndtsson R (1993) Fractal analysis of high-resolution rainfall time series. J Geophys Res: Atmos 98(D12):23265–23274

Ongoma V, Chen H, Omony GW (2018) Variability of extreme weather events over the equatorial East Africa, a case study of rainfall in Kenya and Uganda. Theoret Appl Climatol 131:295–308

Onof C, Chandler RE, Kakou A, Northrop P, Wheater HS, Isham V (2000) Rainfall modelling using Poisson-cluster processes: a review of developments. Stoch Env Res Risk Assess 14:84–411

Overeem A, Buishand A, Holleman I (2008) Rainfall depth-duration-frequency curves and their uncertainties. J Hydrol 348:124–134

Oyoo R, Leemans R, Mol APJ (2011) Future projections of urban waste flows and their impacts in African metropolises cities. Int J Environ Res 5:705–724

Peal A, Evans B, Blackett I, Hawkins P, Heymans C (2014) Fecal sludge management: a comparative analysis of 12 cities. J Water Sanit Hyg Dev 4:563–575

Pfahl S, O'Gorman PA, Fischer EM (2017) Understanding the regional pattern of projected future changes in extreme precipitation. Nat Clim Chang 7:423–427

Requena AI, Burn DH, Coulibaly P (2021a) Technical guidelines for future intensity–duration–frequency curve estimation in Canada. Canadian Water Resources Journal/revue Canadienne Des Ressources Hydriques 46:87–104

Requena AI, Nguyen TH, Burn DH, Coulibaly P (2021b) A temporal downscaling approach for sub-daily gridded extreme rainfall intensity estimation under climate change. J Hydrol: Reg Stud 35:100811

Rodríguez-Solà R, Casas-Castillo MC, Navarro X, Redaño Á (2017) A study of the scaling properties of rainfall in Spain and its appropriateness to generate intensity-duration-frequency curves from daily records. Int J Climatol 37:770–780

Shrestha A, Babel MS, Weesakul S, Vojinovic Z (2017) Developing Intensity–Duration–Frequency (IDF) curves under climate change uncertainty: the case of Bangkok, Thailand. Water 9:145

Silva VLD, Viola MR, Silva DDD, Mello CRD, Pereira SB, Giongo M (2017) Daily rainfall disaggregation for Tocantins State, Brazil. Revista Ambiente & Água 12:605–617

So BJ, Kim JY, Kwon HH, Lima CH (2017) Stochastic extreme downscaling model for an assessment of changes in rainfall intensity-duration-frequency curves over South Korea using multiple regional climate models. J Hydrol 553:321–337

Srivastav RK, Schardong A, Simonovic SP (2014) Equidistance quantile matching method for updating IDF curves under climate change. Water Resour Manag 28:2539–2562

Ssentongo P, Muwanguzi AJ, Eden U, Sauer T, Bwanga G, Kateregga G, Aribo L, Ojara M, Mugerwa WK, Schiff SJ (2018) Changes in Ugandan climate rainfall at the village and forest level. Sci Rep 8:3551

Stratton RA, Senior CA, Vosper SB, Folwell SS, Boutle IA, Earnshaw PD, Kendon E, Lock AP, Malcolm A, Manners J, Morcrette CJ (2018) A pan-African convection-permitting regional climate simulation with the Met Office unified model: CP4-Africa. J Clim 31:3485–3508

Sunyer MA, Luchner J, Onof C, Madsen H, Arnbjerg-Nielsen K (2017) Assessing the importance of spatio-temporal RCM resolution when estimating sub-daily extreme precipitation under current and future climate conditions. Int J Climatol 37:688–705

Svensson C, Olsson J, Berndtsson R (1996) Multifractal properties of daily rainfall in two different climates. Water Resour Res 32:2463–2472

Taylor CM, Lawes EF (1971) Rainfall intensity-duration-frequency data for stations in East Africa. East African Meteorological Department, Technical Memorandum 17, Nairobi

Tfwala CM, van Rensburg LD, Schall R, Mosia SM, Dlamini P (2017) Precipitation intensity-duration-frequency curves and their uncertainties for Ghaap plateau. Clim Risk Manag 16:1–9

Thiery W, Davin EL, Panitz HJ, Demuzere M, Lhermitte S, Van Lipzig N (2015) The impact of the African Great Lakes on the regional climate. J Clim 28:4061–4085

Thiery W, Davin EL, Seneviratne SI, Bedka K, Lhermitte S, van Lipzig NP (2016) Hazardous thunderstorm intensification over Lake Victoria. Nat Commun 7:12786

Thompson JJ, Wilby RL, Matthews T, Murphy C (2022) The utility of Google Trends as a tool for evaluating flooding in data-scarce places. Area 54:203–212

Umer Y, Ettema J, Jetten V, Steeneveld GJ, Ronda R (2021) Evaluation of the WRF model to simulate a high-intensity rainfall event over Kampala Uganda. Water 13:873

Umer Y, Jetten V, Ettema J, Lombardo L (2022) Application of the WRF model rainfall product for the localized flood hazard modeling in a data-scarce environment. Nat Hazards 111:1813–1844

Viney NR, Bates BC (2004) It never rains on Sunday: The prevalence and implications of untagged multi-day rainfall accumulations in the Australian high quality data set. Int J Climatol 24:1171–1192

Wang RQ, Mao H, Wang Y, Rae C, Shaw W (2018) Hyper-resolution monitoring of urban flooding with social media and crowdsourcing data. Comput Geosci 111:139–147

Wells JA, Wilson KA, Abram NK, Nunn M, Gaveau DL, Runting RK, Tarniati N, Mengersen KL, Meijaard E (2016) Rising floodwaters: mapping impacts and perceptions of flooding in Indonesian Borneo. Environ Res Lett 11:064016

Westra S, Fowler HJ, Evans JP, Alexander LV, Berg P, Johnson F, Kendon EJ, Lenderink G, Roberts NM (2014) Future changes to the intensity and frequency of short-duration extreme rainfall. Rev Geophys 52:522–555

Widmann M, Bretherton CS, Salathé EP Jr (2003) Statistical precipitation downscaling over the northwestern United States using numerically simulated precipitation as a predictor. J Clim 16:799–816

Wilby RL (1997) Non-stationarity in daily precipitation series: Implications for GCM down-scaling using atmospheric circulation indices. Int J Climatol 17:439–454

Wilby RL, Dawson CW (2013) The Statistical DownScaling Model (SDSM): Insights from one decade of application. Int J Climatol 33:1707–1719

Wilby RL, Wigley TML (2000) Precipitation predictors for downscaling: observed and General Circulation Model relationships. Int J Climatol 20:641–661

Wilby RL, Wigley TML, Conway D, Jones PD, Hewitson BC, Main J, Wilks DS (1998) Statistical downscaling of General Circulation Model output: a comparison of methods. Water Resour Res 34:2995–3008

Wilby RL, Dawson CW, Barrow EM (2002) SDSM - a decision support tool for the assessment of regional climate change impacts. Environ Model Softw 17:145–157

Wilby RL, Tomlinson OJ, Dawson CW (2003) Multi-site simulation of precipitation by conditional resampling. Clim Res 23:183–194

Wilby RL, Dawson CW, Murphy C, O'Connor P, Hawkins E (2014) The Statistical DownScaling Model—Decision Centric (SDSM-DC): conceptual basis and applications. Clim Res 61:259–276

World Health Organization (WHO) (2018) COP24 special report: health and climate change. World Health Organization, Geneva